Class Based Reconstruction Techniques Using Singular Apparent Contours

G.J.Fletcher and P.J.Giblin

Dept. of Mathematics, University of Liverpool, PO BOX 147, LIVERPOOL, L69 3BX, U.K.

Abstract. We present methods for the *global* reconstruction of some classes of special surfaces. The contour ending (cusp on the apparent contour) is tracked under a dynamic monocular perspective observer. The classes of surfaces considered are surfaces of revolution (SOR), canal surfaces and ruled surfaces. This paper presents theoretical methods for surface reconstruction and error analysis of reconstruction under noise. We find the techniques used exhibit stability even under large noise. This work has added to the accumulating body of work that has arisen in the computer vision community, concerning the differential geometric aspects of special surface classes.

1 Introduction.

We present methods for the *global* reconstruction of some classes of special surfaces by tracking contour endings (cusps) [1] of the apparent contour (also known as the profile and the occluding contour) under a known dynamic monocular perspective observer.

There has been considerable interest in the vision community concerning families of surfaces ([1], [6], [7], [10], [13], [14] for instance). Much of the literature exploits *rich image features*, such as inflections, bitangents, the symmetry set, to aid reconstruction and viewpoint-invariant representation. While there have been some theoretical results concerning the cusps of apparent contours on special surfaces [11],[12], there has been little exploitation of the geometry with regard to reconstruction.

We examine surfaces of revolution (SOR), canal surfaces (piped) and ruled surfaces. Each of these special types of surface is generated in a special way by a moving curve. For example the ruled surface is generated by a sweeping line, the SOR generated by a varying radius circle centred on a straight line and the canal surface is described by sweeping a circle along a space curve, keeping it in the normal plane. (The canal surface can also be considered as an envelope of spheres of constant radius centred along a space curve). If we can recover the generator curve then we recover part of the original surface, even resulting in areas that are unseen and beyond the *frontier* [5]. We recommend [9] for an introduction to the differential geometry of the above classes of surfaces.

[1] We use the terms 'contour ending' and 'cusp' synonymously. A cusp is observed in the image for a transparent surface and for brevity we often refer to 'cusps'.

For each class of surface we provide simulated experiments that illustrate the technique and demonstrate the stability of the reconstruction under extremely noisy data. This simulates the uncertainty in the detection of the contour ending that is present in any practical situation. A contour ending can be seen in Figure 1 where it appears as a dark blob, but the observed location is subject to error.

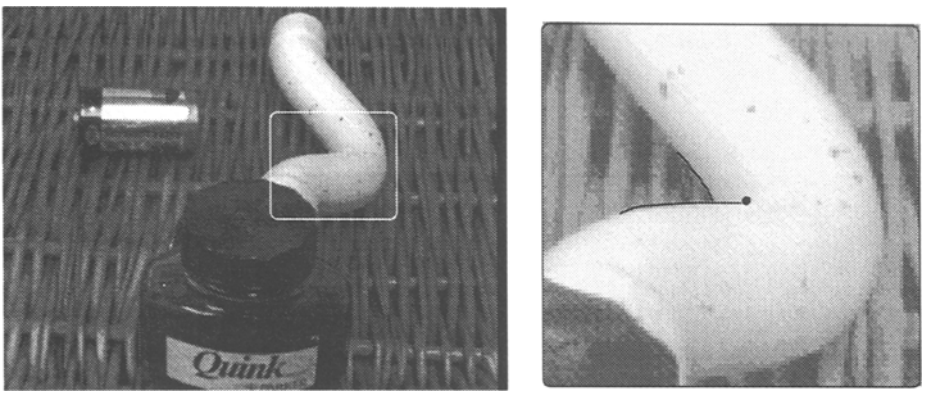

Fig. 1. Canal surface with a T-junction and a contour ending magnified on the right.

2 Background.

For smooth curved surfaces an important image feature is the apparent contour or profile. This is the projection of the locus of points on the surface which separates the visible from occluded parts. Under perspective projection this locus—the contour generator or critical set—can be constructed as the set of points on the surface where rays through the projection centre $\mathbf{c}$ are tangent to the surface. Each viewpoint will generate a different contour generator with the contour generators 'slipping' over the visible surface under viewer motion. This is the familiar situation of [2].

The projection of the contour generator in the image sphere or image plane gives a curve called the apparent contour or profile. This paper is concerned with the situation when the apparent contour ends, or cusps. It is well known (e.g. [8, p.422]) that the apparent contour cusps if and only if the viewing direction is along an *asymptotic direction* and this is equivalent to the view direction being tangent to the contour generator. Recall that a hyperbolic surface patch has two asymptotic directions, and if we extend these directions indefinitely we expect the lines to fill a region of space. Thus any camera position in that region will lie on some asymptotic direction and hence we expect to see cusps in the image.

We recall some results concerning the tracking of cusps from [3].

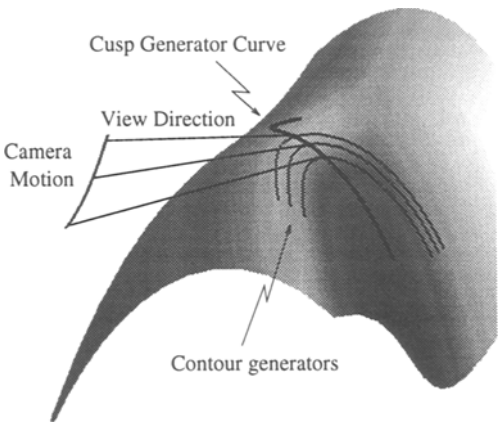

Fig. 2. Cusp generator on a smooth surface.

2.0.1 Definition: *If a point r is on the contour generator and projects in the image to a cusp point then r is said to be a* **cusp generator point**. *As the camera moves the locus of cusp points in the image is the* **cusp locus**, *and the locus of cusp generator points on the surface is the* **cusp generator curve**. *See Figure 2.*

The following proposition informs us that by tracking cusps we can reconstruct a surface strip (i.e. a curve with surface normals) complete with the second fundamental form at the cusp generator points. The main results of this paper concern the extending of this surface strip globally, in a certain sense, for certain classes of surfaces.

As in [3] we consider the camera measurements to be in unrotated *world* coordinates. Using an image sphere with centre $\mathbf{c}$ for mathematical convenience, $\mathbf{c} + \mathbf{p}$ is the position in world coordinates of a point on the apparent contour. The unit vector $\mathbf{p}$ runs from the centre of the sphere to the apparent contour.

2.0.2 Proposition:*[3] If the camera motion is* $\mathbf{c}(t)$, *the cusp generator curve* $\mathbf{r}(t)$, *the cusp locus* $\mathbf{p}(t)$, *the surface normal (equal to the apparent contour normal) at the cusp point* $\mathbf{n}$, *with* $\mathbf{r} = \mathbf{c} + \lambda\mathbf{p}$ *then,*

$$\lambda = -\frac{\mathbf{c}_t.\mathbf{n}}{\mathbf{p}_t.\mathbf{n}}$$

$$K = \frac{-(\mathbf{p}_t.\mathbf{n})^4}{[\mathbf{p}, \mathbf{c}_t, \mathbf{p}_t]^2}$$

$$H = \frac{\mathbf{p}_t.\mathbf{n}(\mathbf{c}_{tt}.\mathbf{n}\ \mathbf{p}_t.\mathbf{n} - \mathbf{c}_t.\mathbf{n}\ \mathbf{p}_{tt}.\mathbf{n} - 2\mathbf{p}.\mathbf{c}_t(\mathbf{p}_t.\mathbf{n})^2)}{2[\mathbf{p}, \mathbf{c}_t, \mathbf{p}_t]^2}$$

where λ *is the depth,* K *is the Gauss curvature and* H *is the Mean curvature, and the suffix denotes differentiation with respect to* t.

A major practical concern is the actual detection of contour endings. Recognising this we provide simulations using large uncertainties in the position in the image of the contour ending, typically ten pixels. We have reported elsewhere [4] of the stability of the formulas in Proposition 2.0.2 under image uncertainty, and the stability is high even under extreme noise.

3 Surfaces of Revolution.

3.1 Theory.

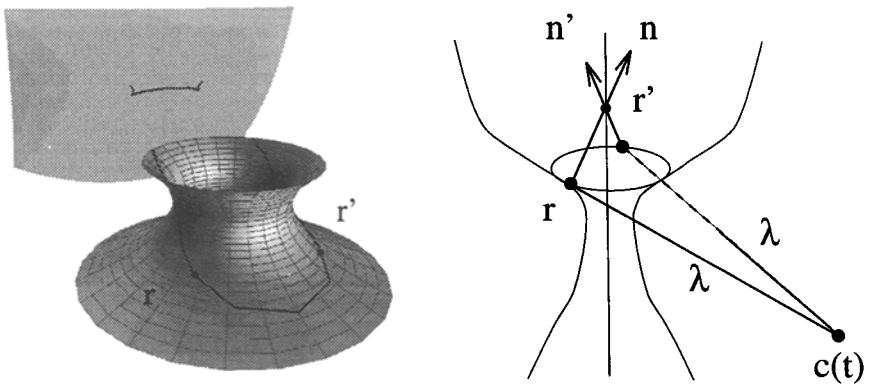

Fig. 3. Left figure: apparent contour (projected on to image sphere) and contour generator (on surface) shown for a particular value of t. Observe the cusp generator pair $\mathbf{r}$ and $\mathbf{r}'$ on the same parallel. Right figure: cusp generator pair $\mathbf{r}$ and $\mathbf{r}'$ on a surface of revolution with surface normals $\mathbf{n}$ and $\mathbf{n}'$ intersecting on the axis.

We now show that by tracking a cusp pair on a surface of revolution (SOR) global information about the surface can be found. More specifically, we assert that by tracking the cusp pair over parallels of our SOR we can reconstruct those parallels. A parallel (section) of a SOR is a plane section of a SOR perpendicular to the axis of rotation. It is a plane circle.

We shall need the following facts.

3.1.1 Fact: *If the point* $\mathbf{r}$ *generates an ordinary cusp for a certain camera position then there exists another point* $\mathbf{r}'$ *on the same parallel with the same depth to the camera that also generates a cusp. Note that the surface at* $\mathbf{r}$ *is congruent to that at* $\mathbf{r}'$*, in particular the Gauss curvatures are equal. See Figure 3.*

This fact tells us that cusps always appear in the image in pairs, and resulting from the same parallel. The following facts will be used in the reconstruction process.

3.1.2 Fact: *The normals to a SOR along a parallel all intersect at a point on the axis, see Figure 3.*

The basic reconstruction technique is as follows.

1. We observe a cusp pair in the image. Note that cusp pairs from the same parallel on the SOR have equal depths and Gauss curvatures by Fact 3.1.1, so we can easily verify from the image which of the cusps we observe do in fact arise from the same parallel.
2. We reconstruct the depth using Proposition 2.0.2 to get two points $\mathbf{r}, \mathbf{r}'$ these are the so-called cusp-generator points.
3. The surface normals are preserved under perspective projection to an image sphere, and so extending the normals at $\mathbf{r}$ and $\mathbf{r}'$ points must give us an intersection on the axis by Fact 3.1.2.
4. Tracking the cusps over time gives us the reconstructed axis.
5. The parallel through $\mathbf{r}$ is then the circle perpendicular to the axis with centre on the axis and passing through $\mathbf{r}$.

As our camera moves the cusp pair sweeps along the parallels and we are able to reconstruct them.

3.2 Experiment.

It is clear that in practice this technique will be susceptible to errors. The image may contain several cusps but it is straightforward to select the correct pair since these cusps arise from points on the surface having the same depth and Gaussian curvature (see Proposition 2.0.2). This provides a consistency check.

In practice when we reconstruct the cusp generator points and extend the normals we find they do not quite intersect. We take the nearest point in this instance and fit an axis to the noisy points.

The reconstruction technique was tested for different amounts of error in the observation of the cusp images. An error of x degrees means that up to x degrees of Gaussian noise was added to the cusp locus on the image sphere to give a noisy locus. For a camera with a focal length of 20mm and pixel density of 500pixels per 5mm, we find that an angular separation of 0.03 degrees is about 1 pixel. For the following SOR experiments errors of 0.3 degrees (10 pixels) and 0.6 degrees (20 pixels) were used.

We now produce some simulated examples which demonstrate the reconstruction technique. The surface used was the following,

$$\mathbf{r}(s,\theta) = ((1+s^2)\cos\theta, (1+s^2)\sin\theta, s)$$

and the camera motion,

$$\mathbf{c}(t) = (10+2t, 0.3t+0.1t^2, -5+4t).$$

Note that the axis of the SOR is the z-axis (0,0,1). We observed a cusp pair at discrete times and added some Gaussian noise of various amounts. This was

then smoothed with a cubic curve via a least-squares method to give the observed cusp loci. The depth was calculated and then the nearest intersection point to the normals was calculated. This gave points on the SOR axis, and a straight axis was fitted. The parallels could then be generated resulting in a radius function that could then be smoothed giving a complete SOR.

We now illustrate some of the results for an error of 0.3 degrees and 0.6 degrees. The reconstructed axis for an error of 0.3 degrees was calculated as $[.051-.001u, -.013+.003u, -1.198+.999u]$, recall that the actual axis is $[0, 0, u]$. The axis for 0.6 degrees is $[.158-.012u, -.074+.013u, -1.142+.999u]$. See Figure 4.

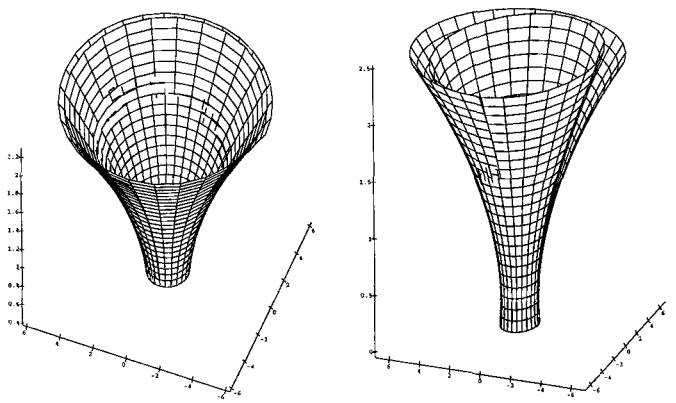

Fig. 4. Actual surface (cut away) compared with recovered surface (0.3degs) (left). Actual surface (cut away) compared with reconstructed surface (0.6 degs) (right).

4 Canal Surfaces.

4.1 Theory

Let $\gamma(t)$ be a space curve and $N(t)$ be its principal normal and $B(t)$ be the binormal. Then the standard parameterisation for a canal surface is the following:

$$\mathbf{r}(t, \theta) = \gamma(t) + r(N(t)\cos\theta + B(t)\sin\theta).$$

We can also think of the canal surface as an envelope of a family of spheres of radius r centred on $\gamma(t)$.

4.1.1 Definitions. *The space-curve* γ *is the* **core curve**, *the factor* r *is the (constant)* **radius** *of the canal surface. The circle* $\gamma(t_0)+r(N(t_0)\cos\theta+B(t_0)\sin\theta)$ *is the* **characteristic circle** *for* $t = t_0$.

We assert that by tracking a single cusp along the canal surface we can reconstruct the characteristic circles (and hence the complete surface) as the cusp sweeps along the surface. We note that this reconstruction technique works with incomplete viewer information, such as when only one 'side' of the canal surface is visible. We shall need the following fact.

4.1.2 Fact:

1. *The radius of a canal surface can be expressed in terms of the Gaussian curvature K, and the Mean curvature H, as $r = \frac{H-\sqrt{H^2-K}}{K}$.*
2. *The normal to a canal surface at a point p passes through the centre of the characteristic circle of p.*

Recall that we can calculate K and H from tracking cusps using Proposition 2.0.2 and so can recover the radius. The reconstruction technique is as follows,

1. Track cusp to recover depth, Gaussian and Mean curvature.
2. Calculate the radius r via 4.1.2.
3. Using the recovered depth we can recover the cusp generator point and then move along the normal a distance r to recover the core curve by 4.1.2.
4. The core curve and radius completely determine the canal surface.

4.2 Experiment.

We simulate the reconstruction process with a simple example. Again noise will be added to the image of the cusp points to simulate the uncertainty in detecting the cusp points. Figure 5 shows the cusp points on the image sphere in theta/phi coordinates. The core-curve used will be, $\gamma(t) = (2t, 0.6t^2, 0)$ and the radius 1. Note that the core curve of this canal surface is planar; this is just to simplify the calculations and does not imply a restriction inherent in the technique used. An error of 0.5 degrees was added in this example and the recovered radius was 0.973. It is difficult to quantify the error in the core curve, but Figure 6 shows the actual and recovered core curves. The recovered and actual surfaces are shown in Figure 6. It is unclear how best to empirically measure the 'success' of the reconstruction, other than simply a visual inspection. Figure 7 shows a series of experiments performed on different canal surfaces all with radius one, and varying camera motions. The horizontal axis indicates increasing noise added, and the vertical axis shows the recovered radius. A deviation from a radius equal to one, shows the effect of the noise. We don't expect this relationship to be simple since the radius depends on second derivatives of the cusp locus (Fact 4.1.2). We merely wish to assess the stability under large noise.

5 Ruled surfaces.

5.1 Theory.

We now consider tracking a cusp on a ruled surface. As the cusp sweeps across the rulings we find that we are able to reconstruct the rulings and hence the

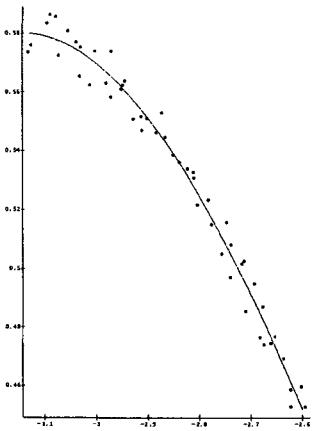

Fig. 5. Image of noisy cusp points with a cubic curve fitted.

whole surface. The crucial observation is contained in the following fact from [8, p.361].

5.1.1 Fact: *If the angle between asymptotic directions at a hyperbolic point of a surface is* ϕ*, then* $\tan\phi = \frac{\sqrt{-K}}{H}$.

By tracking cusps we can recover K, H, the depth, the surface normal and one asymptotic direction (namely the view direction). Recall that for a ruled surface one asymptotic direction is always along the ruling and $K \leq 0$. The ingredients are now all present along with Fact 5.1.1, and the recipe is now given.

1. Track cusp and recover the depth, K and H.
2. The view direction is one asymptotic direction and the other is the ruling. Calculate the angle between them by Fact 5.1.1 and since we know that the ruling lies in the tangent plane this constrains it.
3. This gives the direction of the ruling, and it passes through the cusp generator point which can be recovered with knowledge of the depth.

Figure 7 shows the result of a reconstruction experiment on a ruled surface where the maximum Gaussian error in observed cusp points was 0.3 degrees.

6 Conclusion

We have shown that the cusps on the apparent contours of certain classes of smooth surfaces give enough information to enable the *complete* reconstruction of the surface by tracking cusps alone. This work has built on the theory developed in [3].

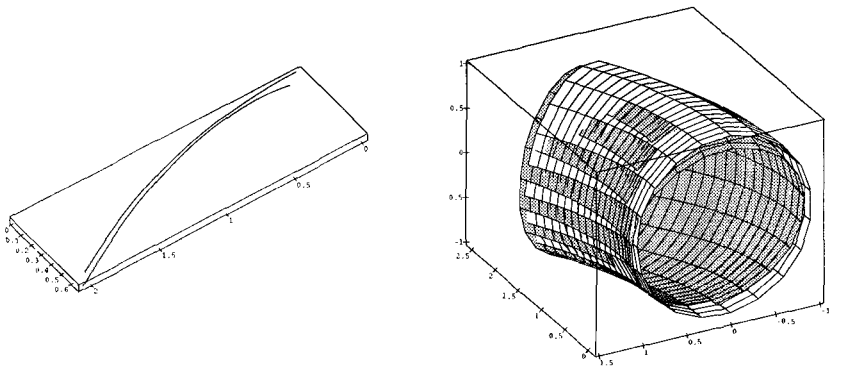

Fig. 6. Actual and recovered core curves (left), and actual and recovered surfaces (right). Note that the scale and orientation are different on left and right.

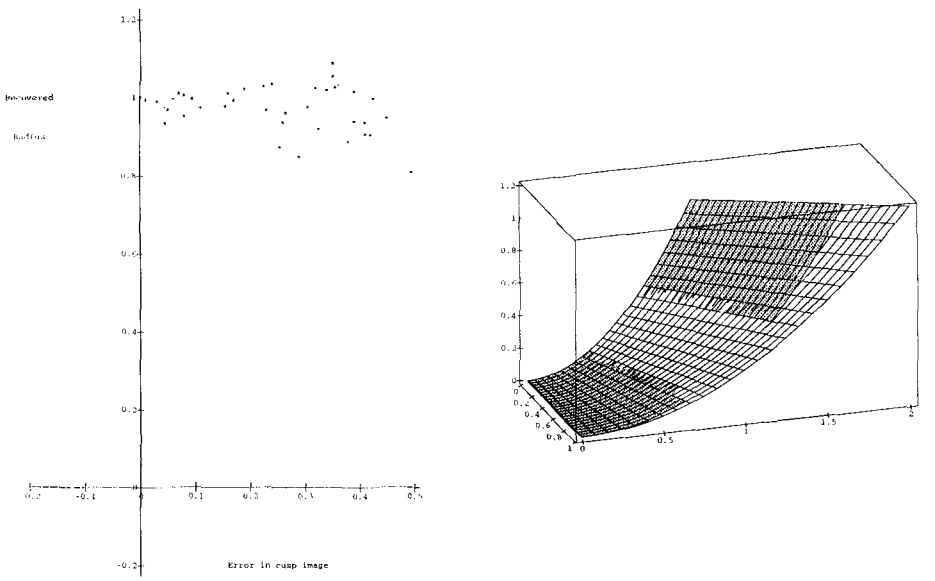

Fig. 7. Left figure: increase in maximum angular error of cusp points (horizontal) with recovered radius of canal surface (vertical). Right figure: actual and reconstructed ruled surface with an error of 0.3 degrees.

Recognising that cusps are hard to detect in real images we have given an error analysis that demonstrates the stability of the reconstruction even under large image perturbation.

Future work will include extending the methods to other classes of special surfaces, and the analysis of real image data.

Acknowledgements: we thank Dr.R.Morris for his software 'The Liverpool Software Modelling Package' that produced Figure 2 and Figure 3 and Dr.A.Zisserman for Figure 1.

We also acknowledge support through grant GR/H59855 from the British research council EPSRC (formerly SERC). The first author is supported by EPSRC.

References

1. J.W.Bruce, P.J.Giblin, F.Tari, 'Special surfaces and their duals; preliminary version', *Liverpool University Preprint.* (1995).
2. R.Cipolla and A.Blake, 'Surface shape from deformation of apparent contours', *Int. J. of Computer Vision* 9 (1992), 83-112.
3. R.Cipolla, G.Fletcher, P.Giblin, 'Surface geometry from cusps of apparent contours', *Proc. Fifth Int. Conf. on Computer Vision*, Cambridge, Mass, June 1995, pp.858-863.
4. R.Cipolla, G.Fletcher, P.Giblin, 'Following Cusps', *to appear in Int.J.Computer Vision.*
5. R.Cipolla, K.E.Åström and P.J.Giblin, 'Motion from the frontier of curved surfaces', *Proc. Fifth Int. Conf. on Computer Vision*, Cambridge, Mass, June 1995, pp.269-275
6. D.A.Forsyth, J.L.Mundy, A.Zisserman, C.A.Rothwell, 'Recognising rotationally symmetric surfaces from their outlines', *Proc. Second European Conf. on Computer Vision*, Santa Margherita Ligure (Italy), pp.639-647, May 1992.
7. R.Glachet, M.Dhome, J.T.Lapreste, 'Finding the pose of an object of revolution', *Proc. Second European Conf. on Computer Vision*, Santa Margherita Ligure (Italy), pp.681-686, May 1992.
8. J.J.Koenderink, *Solid Shape*, M.I.T.Press 1990.
9. B. O'Neill, *Elementary Differential Geometry*, Academic Press 1966.
10. J.Ponce, 'Invariant properties of straight homogeneous generalized cylinders'. *IEEE PAMI*, vol.11,no.9,pp.951-965,1989.
11. J.Ponce, D.Chelberg, 'Finding the limbs and cusps of Generalized Cylinders.' *Int. J.Comp. Vision 1*, (1987) 195-210.
12. J.H.Rieger,'Projections of generic surfaces of revolution', *Geometriae Dedicata*, 1993, Vol.48, No.20, pp.211-230.
13. A.Zisserman, J.Mundy, D.Forsyth, J.Liu, N.Pillow, C.Rothwell and S.Utcke, 'Class-Based Groupings in Perspective Images', *Proc. Fifth Int. Conf. on Computer Vision*,Cambridge, Mass, June 1995.
14. M.Zerroug, R.Nevatia, 'Segmentation and recovery of SHGCs from a real intensity image.', *Proc. Third European Conf. on Computer Vision*, Stockholm, Sweden Vol.I pp.319-330, May 1994.